

Two identities for Poisson Point Processes and Voronoi Tessellations with Applications

Mohsen Amidzadeh

Department of Computer Science, Aalto University, Finland

Abstract—In this paper, we introduce two identities—one pertaining to the state space of Poisson Point Processes (PPPs), and the other for the Voronoi tessellations formed by PPPs. Then, we explore several applications of these identities within the context of wireless cellular networks.

Index Terms—Poisson Point Process, Voronoi Tessellation, Cellular Networks.

I. INTRODUCTION

Stochastic geometry is considered a versatile tool for modeling and analyzing wireless cellular networks, both for homogeneous and Heterogeneous Networks (HetNets) [1]–[11]. In the context of caching at the wireless edge, Poisson Point Processes (PPPs) have been used to model deployment of BSs and locations of UE in [12]–[16]. In [12], where BSs apply a beamforming content delivery and the expected ergodic spectral efficiency is optimized, stochastic geometry is used to model BS deployment. In [17], optimum cache policies are found in HetNets modelled based on independent PPPs. In [13], two independent PPPs are exploited to model the deployment of two tiers of a HetNets. Aiming to find an optimal cache placement policy, independent PPPs are exploited in [14] to obtain an expression for the successful transmission probability in a HetNet. In [15], the coverage probability is approximated using PPP for the multi-antenna small-cell networks to design an optimal cache placement policy. In [16], the authors leverage PPP to optimize the minimum of the cache hit rates of different request-related categorized UEs. [8]–[10] apply stochastic geometry to demonstrate that the probabilistic cache policies significantly improves the quality-of-service. [11] presents a compound cache policy schemes with performance analysis done by the aid of stochastic geometry. These studies highlight the applicability of stochastic geometry in analysis the performance metrics of cellular networks. In this paper we present two identities for the Voronoi tessellations constructed of Poisson Point Processes, and provide some applications of these identities in the context of mobile cellular networks. This work provide a versatile analytical tool for analyzing the conventional transmission schemes of the wireless networks using the stochastic geometry.

The remainder of this paper is organized as follows. In Section II, we present two identities related to Poisson point processes. In Section III, we discuss about the applications of these identities. Section IV then concludes the paper.

Notations: We use lower-case a for scalars, bold-face lower-case \mathbf{a} for vectors and bold-face uppercase \mathbf{A} for matrices. $\|\mathbf{a}\|$

is the Euclidean norm of \mathbf{a} , $\{a_n\}_n$ collects the components of vector \mathbf{a} and $\mathbb{1}(\cdot)$ is the indicator function.

II. AN IDENTITY FOR POISSON-VORONOI TESSELLATIONS

We now present the first identity in the following Lemma.

Lemma 1. *Let $\{\mathbf{x}_i\}_{i \in \Phi_1}$ be the points of a homogeneous PPP Φ_1 with intensity λ_1 , and $S(\cdot)$ and $P(\cdot)$ be two real-valued functions on the state space of Φ_1 . We then have:*

Identity 1: Expectation of sum-product of functions on the state space of PPP.

$$\mathbb{E} \left\{ \prod_{k \in \Phi_1} P(\mathbf{x}_k) \sum_{k \in \Phi_1} S(\mathbf{x}_k) \right\} = \lambda_1 \iint_{\mathbb{R}^2} S(\mathbf{s}) P(\mathbf{s}) d\mathbf{s} \exp \left(\lambda_1 \iint_{\mathbb{R}^2} (P(\mathbf{s}) - 1) d\mathbf{s} \right)$$

Proof. please refer to Appendix A for the proof. \square

The second identity is presented as follows.

Lemma 2. *Assume $\{\mathbf{r}_i\}_{i \in \Phi_2}$ to be the Poisson points located based on a PPP Φ_2 , and consider Voronoi tessellation constructed by these points with \mathcal{V}_0 being the Voronoi cell associated with \mathbf{r}_0 , then the quantity $\mathbb{1}(\mathbf{x} \in \mathcal{V}_0)$, for any location $\mathbf{x} \in \mathbb{R}^2$, can be expressed based on the following function product in Φ_2 :*

Identity 2: Expression of $\mathbb{1}(\mathbf{x} \in \mathcal{V}_0)$ based on a product of functions.

$$\mathbb{1}(\mathbf{x} \in \mathcal{V}_0) = \prod_{k \in \Phi_2 \setminus \{0\}} \mathbb{1}(\mathbf{x} \in M_0(\mathbf{r}_k)), \quad (1)$$

where $\mathbb{1}(\cdot)$ is the indicator function and

$$M_0(\mathbf{r}_k) := \{\mathbf{r}' \in \mathbb{R}^2 \mid \|\mathbf{r}' - \mathbf{r}_0\| \leq \|\mathbf{r}' - \mathbf{r}_k\|\}. \quad (2)$$

Moreover, for the space $\{\mathbf{r} \in \mathbb{R}^2 \mid \mathbf{x} \in M_0(\mathbf{r})\}$ with a given $\mathbf{x} \in \mathbb{R}^2$, we have:

$$\{\mathbf{r} \in \mathbb{R}^2 \mid \mathbf{x} \in M_0(\mathbf{r})\} = B_c(\mathbf{r}; \mathbf{x}, \|\mathbf{x}\|),$$

where $B_c(\mathbf{r}; \mathbf{x}, \|\mathbf{x}\|)$ defines the space exterior to the circle centered at \mathbf{x} with a radius of $\|\mathbf{x}\|$.

Proof. please refer to Appendix B for the proof. \square

Remark 1. Consider $\{\mathbf{x}_i\}_{i \in \Phi_1}$ and $\{\mathbf{r}_i\}_{i \in \Phi_2}$ as Poisson points of two independent PPPs Φ_1 and Φ_2 with intensities λ_1 and λ_2 , respectively, and \mathcal{V}_0 being the Voronoi cell associated with \mathbf{r}_0 , and $P(\cdot)$ a real-valued function on the state space of Φ_1 . Then, we have:

$$\mathbb{E} \left\{ \sum_{k \in \mathcal{V}_0} P(\mathbf{x}_k) \right\} = \lambda_1 \iint_{\mathbb{R}^2} P(\mathbf{x}) \exp(-\pi \lambda_2 \|\mathbf{x}\|^2) d\mathbf{x},$$

and

$$\mathbb{E} \left\{ \prod_{k \in \mathcal{V}_0} P(\mathbf{x}_k) \right\} = \exp \left(\lambda_1 \iint_{\mathbb{R}^2} (P(\mathbf{x}) \exp(-\pi \lambda_2 \|\mathbf{x}\|^2) - 1) d\mathbf{x} \right).$$

Proof. See Appendix C for the proof. \square

III. APPLICATIONS

In the following sections, we present two applications of developed identities for analyzing network performance within cellular networks.

A. Average Number of UEs within a Voronoi Cell

We here intend to use Lemma 2 to compute the average number of UEs within a Voronoi Cell of BSs. This is an important parameter since each UE is served by its nearest BS in the conventional transmission scheme of cellular network.

For this, consider BSs and UEs which are located based on two independent PPPs, Φ_u and Φ_b with intensities λ_u and λ_b . We denote the location of BSs and UEs by $\{\mathbf{r}_i\}_{i \in \Phi_b}$ and $\{\mathbf{x}_i\}_{i \in \Phi_u}$, respectively. The BSs constitutes a Voronoi tessellation with different cells denoted by $\{\mathcal{V}_i\}_i$. Notice that the PDF of cell size of Voronoi tessellation is accurately approximated by a gamma distribution with shape K and scale $1/(K\lambda_b)$ [18], [19] with $K = 3.575$. This gives the average cell size equal to $\bar{A} = K \frac{1}{K\lambda_b} = \frac{1}{\lambda_b}$. Therefore, the average number of UEs within a typical Voronoi cell \bar{n}_u can be approximated as follows:

$$\bar{n}_u = \lambda_u \bar{A} = \frac{\lambda_u}{\lambda_b}. \quad (3)$$

We now intend to verify this quantity using Lemma 2. Without loss of generality, we can compute \bar{n}_u for \mathcal{V}_0 .

$$\begin{aligned} \bar{n}_u &= \mathbb{E} \left\{ \sum_{i \in \Phi_u} \mathbb{1}(\mathbf{x}_i \in \mathcal{V}_0) \right\} \\ &\stackrel{(a)}{=} \mathbb{E}_{\Phi_b} \mathbb{E}_{\Phi_u} \left\{ \sum_{i \in \Phi_u} \prod_{k \in \Phi_b \setminus \{0\}} \mathbb{1}(\mathbf{x}_i \in M_0(\mathbf{r}_k)) \right\} \\ &\stackrel{(b)}{=} \mathbb{E}_{\Phi_u} \left\{ \sum_{i \in \Phi_u} \exp \left(\lambda_b \iint_{\mathbb{R}^2} (\mathbb{1}(\mathbf{x}_i \in M_0(\mathbf{r})) - 1) d\mathbf{r} \right) \mid \Phi_b \right\} \\ &\stackrel{(c)}{=} \mathbb{E}_{\Phi_u} \left\{ \sum_{i \in \Phi_u} \exp \left(\lambda_b \iint_{B_c(\mathbf{r}; \mathbf{x}_i, \|\mathbf{x}_i\|)} 1 d\mathbf{r} - \lambda_b \iint_{\mathbb{R}^2} 1 d\mathbf{r} \right) \mid \Phi_b \right\} \\ &\stackrel{(d)}{=} \lambda_u \iint_{\mathbb{R}^2} \exp \left(\lambda_b \iint_{B_c(\mathbf{r}; \mathbf{x}, \|\mathbf{x}\|)} 1 d\mathbf{r} - \lambda_b \iint_{\mathbb{R}^2} 1 d\mathbf{r} \right) x dx d\theta \\ &= \lambda_u \iint_{\mathbb{R}^2} \exp(-\lambda_b \pi x^2) x dx d\theta = \frac{\lambda_u}{\lambda_b}, \end{aligned} \quad (4)$$

where $x = \|\mathbf{x}\|$ and $r = \|\mathbf{r}\|$. Furthermore, for (a) we used the Lemma 2, for (b) we leveraged Campbell's Theorem [21] for Φ_b , and for (c), we used

$$\{\mathbf{r} \in \mathbb{R}^2 \mid \mathbf{x} \in M_0(\mathbf{r})\} = B_c(\mathbf{r}; \mathbf{x}, \|\mathbf{x}\|),$$

from Lemma 2 with $B_c(\mathbf{r}; \mathbf{x}, \|\mathbf{x}\|)$ denoting the space outside the circle centered at \mathbf{x} with a radius of $\|\mathbf{x}\|$. Moreover, for (d), Campbell's Theorem was now used for Φ_u . The obtained result interestingly confirms the approximation obtained in Eq. (3).

B. Total Bandwidth Consumption

In this section we use Lemmas 1 and 2 to compute the total bandwidth consumption of the conventional unicast scheme [22]–[24] within the cellular networks. For this, consider a network with BSs applying the conventional single-point unicast scheme to serve the requesting UEs of the network. Each UE of this transmission scheme requests the needed content from its nearest BS. We consider the transmission rate R for the content requests of UEs. Therefore, this scheme develops an on-demand transmission with BS-specific association. Each BS uses the full bandwidth W for content delivery, i.e., frequency reuse 1 is used [25]. This is according to the concurrent standards of mobile networks [25]–[27].

The locations of UEs and BSs are considered based on two independent PPPs, Φ_u and Φ_b , respectively, and with intensities λ_u and λ_b .

Since each UE is served by its nearest BS, they establish a Voronoi tessellation with different cell size. As such, there may be U distinct UEs requesting from the BS of a typical Voronoi cell. For UE k served by the network, the SINR is:

$$\gamma_k = \frac{|h_0^k|^2 \|\mathbf{x}_k - \mathbf{r}_0\|^{-e}}{1/\gamma_{\text{tx}} + \underbrace{\sum_{j \in \Phi_b \setminus \{0\}} |h_j^k|^2 \|\mathbf{x}_k - \mathbf{r}_j\|^{-e}}_{I_k}}, \quad (5)$$

where the Tx-SNR is $\gamma_{\text{tx}}^{\text{UC}} = p_{\text{tx}}/(WN_0)$ with p_{tx} being the average transmission power of BSs. Moreover, e is the path-loss component, h_0^k is the channel coefficient between nearest BS and UE k , and h_j^k is the channel coefficient from BS j to UE k . We use a standard distance-dependent path-loss model, and assume a Rayleigh distribution for the channel coefficient, i.e., $|h_{j,k}|^2 \sim \exp(1)$.

Within each cell, the BS follows a UE-specific resource allocation policy to ensure an adequate allotment of resources for the served UEs. However, when the SINR of a UE diminishes significantly, near infinite bandwidth is required to serve the UE. To address this challenge, it is conventional [28] to implement a truncated SINR strategy, wherein the bandwidth allocated to serve UE k is:

$$w_k^{\text{UC}} = \begin{cases} R/\log_2(1 + \gamma_k^{\text{UC}}), & \gamma_k^{\text{UC}} \geq \gamma \\ 0, & \text{otherwise} \end{cases}, \quad (6)$$

where γ is the SINR threshold and R represents the desired transmission rate. Consequently, no resources are utilized if the UE experiences poor fading situation.

We make the assumption that each BS serves all of its U associated UEs, with the necessary radio resources allocated to fulfill their requirements. Consequently, the resource consumption within each cell is determined by the total resources allocated to the UEs within that cell. Furthermore, we assume that all BSs remain active during network transmissions, thereby the average resource consumption is determined by the average consumption of a typical Voronoi cell \mathcal{V}_0 :

$$W(\cdot) = \mathbb{E} \left\{ \sum_{k \in \mathcal{V}_0} w_k^{\text{UC}} \right\}. \quad (7)$$

Note that the expectation is with respect to Φ_u and Φ_b , as well as with respect to the channel coefficients, based on (5). For the network-wide resource consumption, we then have:

Theorem 1. *Assume an interference-limited frequency reuse 1 cellular network, wherein every UE is served by its nearest BS. The position of BSs and UEs adhere to PPPs with intensities λ_b and λ_u , respectively. BSs allocate bandwidth to UEs using SINR service threshold γ as outlined in (6). The average of required resources across whole network is then:*

$$W(\gamma) = \frac{\lambda_u}{\lambda_b} \int_0^{w_{\text{th}}} w \frac{d}{dw} \left(\frac{\eta(w) - \gamma}{\eta(w)T(\eta(w)) - \gamma T(\gamma)} \right) dw, \quad (8)$$

where $w_{\text{th}} = \frac{R}{\log_2(1 + \gamma)}$ and $T(x) = 1 + \sqrt{x} \tan^{-1}(\sqrt{x})$ and $\eta(w) = 2^{\frac{R}{w}-1}$.

Proof. First, we need to calculate the expected resources required by a typical User Equipment (UE) requesting services from the network. Based on (5) and (6) and by defining $w_k = \frac{R}{\log(1 + \gamma_k)}$, we get:

$$\begin{aligned} \mathbb{E}_{\gamma_k} \left\{ \frac{R}{\log(1 + \gamma_k)} \mathbb{1}(\gamma_k \geq \gamma) \right\} &= \mathbb{E}_{w_k} \left\{ \frac{R}{\log(1 + \gamma_k)} \mathbb{1}(w_k \leq w_{\text{th}}) \right\} \\ &= \mathbb{E}_{w_k} \left\{ \frac{R}{\log(1 + \gamma_k)} \mid w_k \leq w_{\text{th}} \right\} \Pr(w_k \leq w_{\text{th}}) \\ &= \int_0^{w_{\text{th}}} w \frac{d}{dw} F_{w_k}(w) dw F_{w_k}(w_{\text{th}}), \end{aligned} \quad (9)$$

where $w_{\text{th}} = R/\log(1 + \gamma)$, and $F_{w_k}(w)$ is the cumulative density function (CDF) of r.v. w_i evaluated at w , Based on (5), we then obtain:

$$\begin{aligned} F_{w_k}(w) &= 1 - \mathbb{P} \{ |h_0^k|^2 \|\mathbf{x}_k\|^{-e} \leq I_k \eta(w) \} \\ &\stackrel{(a)}{=} \mathbb{E}_{I_k} \{ \exp(-\eta(w) I_k \|\mathbf{x}_k\|^e) \}, \end{aligned}$$

where $\eta(w) = 2^{\frac{R}{w}-1}$, and (a) is obtained based on $|h_0^k|^2 \sim \exp(1)$. Considering that $I_k = \sum_{j \in \Phi_b \setminus \{0\}} |h_j^k|^2 \|\mathbf{x}_k - \mathbf{r}_k\|^{-e}$ and $|h_j^k|^2 \sim \exp(1)$, we can get:

$$\begin{aligned} \mathbb{E}_{I_k} \{ \exp(-\eta(w) I_k \|\mathbf{x}_k\|^e) \} &= \prod_{j \in \Phi_b} \left(1 + \eta(w) \frac{\|\mathbf{x}_k - \mathbf{r}_j\|^{-e}}{\|\mathbf{x}_k\|^{-e}} \right)^{-1} \\ &= \prod_{j \in \Phi_b} P_w \left(\frac{\|\mathbf{x}_k - \mathbf{r}_j\|^{-e}}{\|\mathbf{x}_k\|^{-e}} \right), \end{aligned}$$

where $P_w(\zeta) := (1 + \eta(w)\zeta)^{-1}$. Therefore, we get:

$$F_{w_k}(w) = \prod_{j \in \Phi_b} P_w \left(\frac{\|\mathbf{x}_k - \mathbf{r}_j\|^{-e}}{\|\mathbf{x}_k\|^{-e}} \right).$$

By using $\frac{d}{dw} F_{w_k}(w) = F_{w_k}(w) \frac{d}{dw} \log(F_{w_k}(w))$, and defining

$$S_w(\zeta) := -\frac{d\eta(w)}{dw} \frac{\zeta}{1 + \eta(w)\zeta},$$

we can obtain:

$$\begin{aligned} \mathbb{E}_{\gamma_k} \left\{ \frac{R}{\log(1 + \gamma_k)} \mathbb{1}(\gamma_k \geq \gamma) \right\} &= \int_0^{w_{\text{th}}} w \sum_{j \in \Phi_b} S_w \left(\frac{\|\mathbf{x}_k - \mathbf{r}_j\|^{-e}}{\|\mathbf{x}_k\|^{-e}} \right) \prod_{j \in \Phi_b} P_w \left(\frac{\|\mathbf{x}_k - \mathbf{r}_j\|^{-e}}{\|\mathbf{x}_k\|^{-e}} \right) dw \\ &\quad \times \prod_{j \in \Phi_b} P_{w_{\text{th}}} \left(\frac{\|\mathbf{x}_k - \mathbf{r}_j\|^{-e}}{\|\mathbf{x}_k\|^{-e}} \right). \end{aligned} \quad (10)$$

We now present the main part of the proof of Theorem 1. For this, we compute $W(\gamma) = \mathbb{E} \{ \sum_{k \in \mathcal{V}_0} w_k \}$ from (7). According to Slivnyak-Make theorem [20], we assume that the BS responsible of cell \mathcal{V}_0 is located at origin, i.e., $\mathbf{r}_0 = \mathbf{0}$. Based on (5), we have:

$$\begin{aligned} W(\gamma) &= \mathbb{E}_{\Phi_u, \Phi_b} \mathbb{E}_{\gamma} \left\{ \sum_{k \in \mathcal{V}_0} \frac{R}{\log(1 + \gamma_k)} \mathbb{1}(\gamma_k \geq \gamma) \right\} \\ &= \mathbb{E}_{\Phi_u, \Phi_b} \left\{ \sum_{k \in \Phi_u} \mathbb{E}_{\gamma_k} \left\{ \frac{R}{\log(1 + \gamma_k)} \mathbb{1}(\gamma_k \geq \gamma) \right\} \mathbb{1}(\mathbf{x}_k \in \mathcal{V}_0) \right\} \\ &\stackrel{(a)}{=} \mathbb{E}_{\Phi_u} \left\{ \sum_{k \in \Phi_u} \mathbb{E}_{\Phi_b} \left\{ \int_0^{w_{\text{th}}} w \sum_{j \in \Phi_b \setminus \{0\}} S_w \left(\frac{\|\mathbf{x}_k - \mathbf{r}_j\|^{-e}}{\|\mathbf{x}_k\|^{-e}} \right) \mathbb{1}(\mathbf{x}_k \in M_0(\mathbf{r}_j)) \right. \right. \\ &\quad \left. \left. \times \prod_{j \in \Phi_b \setminus \{0\}} P_w \left(\frac{\|\mathbf{x}_k - \mathbf{r}_j\|^{-e}}{\|\mathbf{x}_k\|^{-e}} \right) P_{w_{\text{th}}} \left(\frac{\|\mathbf{x}_k - \mathbf{r}_j\|^{-e}}{\|\mathbf{x}_k\|^{-e}} \right) \mathbb{1}(\mathbf{x}_k \in M_0(\mathbf{r}_j)) dw \right\} \right\} \end{aligned} \quad (12)$$

where for (a) we use (10) and Lemma 2. In (12) we are dealing with a reduced-palm process as $j \in \Phi_b \setminus \{0\}$. Considering that the distribution of reduced-palm process is equal to the distribution of original process [20], and based on Lemma 1, we obtain (11) which is written in the top of next page, where $Q_w(\cdot) := S_w(\cdot)P_w(\cdot)P_{w_{\text{th}}}(\cdot)$. By following Lemma 2 that

$$\{ \mathbf{r} \in \mathbb{R}^2 \mid \mathbf{x} \in M_0(\mathbf{r}) \} = B_c(\mathbf{r}; \mathbf{x}, \|\mathbf{x}\|),$$

we then get:

$$\begin{aligned} W(\gamma) &= \int_0^{w_{\text{th}}} w \lambda_b \lambda_u \iint_{\mathbb{R}^2} \left\{ \iint_{B_c(\mathbf{r}; \mathbf{x}, \|\mathbf{x}\|)} Q_w \left(\frac{\|\mathbf{x} - \mathbf{r}\|^{-e}}{\|\mathbf{x}\|^{-e}} \right) r dr d\theta \right. \\ &\quad \times \exp \left(\lambda_b \iint_{B_c(\mathbf{r}; \mathbf{x}, \|\mathbf{x}\|)} P_w \left(\frac{\|\mathbf{x} - \mathbf{r}\|^{-e}}{\|\mathbf{x}\|^{-e}} \right) P_{w_{\text{th}}} \left(\frac{\|\mathbf{x} - \mathbf{r}\|^{-e}}{\|\mathbf{x}\|^{-e}} \right) r dr d\theta \right. \\ &\quad \left. \left. - \lambda_b \iint_{\mathbb{R}^2} r dr d\theta \right) \right\} x dx d\theta' dw, \end{aligned} \quad (13)$$

where $x = \|\mathbf{x}\|$. Note that (13) obtained by considering the probability generating functional (PGFL) property of PPP Φ_u

$$\begin{aligned}
W(\gamma) &= \int_0^{w_{\text{th}}} w \mathbb{E}_{\Phi_u} \left\{ \sum_{k \in \Phi_u} \lambda_b \iint_{\mathbb{R}^2} Q_w \left(\frac{\|\mathbf{x}_k - \mathbf{r}\|^{-e}}{\|\mathbf{x}_k\|^{-e}} \right) \mathbb{1}(\mathbf{x}_k \in M_0(\mathbf{r})) r dr d\theta \right. \\
&\quad \left. \times \exp \left(\lambda_b \iint_{\mathbb{R}^2} \left(P_w \left(\frac{\|\mathbf{x}_k - \mathbf{r}\|^{-e}}{\|\mathbf{x}_k\|^{-e}} \right) P_{w_{\text{th}}} \left(\frac{\|\mathbf{x}_k - \mathbf{r}\|^{-e}}{\|\mathbf{x}_k\|^{-e}} \right) \mathbb{1}(\mathbf{x}_k \in M_0(\mathbf{r})) - 1 \right) r dr d\theta \right) \right\} dw,
\end{aligned} \tag{11}$$

[20]. Now, we consider change of variables $\boldsymbol{\rho} = \mathbf{x} - \mathbf{r}$, and then $\mathbf{q} = z\boldsymbol{\rho}$ to obtain:

$$\begin{aligned}
W(\gamma) &= \int_0^{w_{\text{th}}} w \lambda_b \lambda_u \iint_{\mathbb{R}^2} \left\{ 2\pi \int_1^\infty Q_w(z^{-e}) q^2 z dz \right. \\
&\quad \left. \times \exp \left(2\pi \lambda_b q^2 \left(\int_1^\infty P_w(z^{-e}) P_{w_{\text{th}}}(z^{-e}) z dz - \int_0^\infty z dz \right) \right) \right\} q dq dw \\
&\stackrel{(a)}{=} \int_0^{w_{\text{th}}} \left(\frac{\lambda_u}{2\lambda_b} w \int_1^\infty Q_w(z^{-e}) z dz \Omega_1^2(w) \right) dw \\
&= \frac{\lambda_u}{2\lambda_b} \int_0^{w_{\text{th}}} w \frac{d}{dw} \Omega_w(w) dw,
\end{aligned}$$

where

$$\Omega_w(w) = \frac{1}{\frac{1}{2} - \int_1^\infty (P_w(z^{-e}) P_{w_{\text{th}}}(z^{-e}) - 1) z dz},$$

$\rho = \|\boldsymbol{\rho}\|$, $q = \|\mathbf{q}\|$, $\frac{d}{dw} P_w(\cdot) P_{w_{\text{th}}}(\cdot) = Q_w(\cdot)$ and for (a) we use $\int_0^\infty q^3 \exp(\phi_0 q^2) dq = \frac{1}{2\phi_0^2}$ for $\phi_0 < 0$. By computing the inner integral for $e = 4$, the statement follows. \square

Remark: For the case of service threshold $\gamma \rightarrow 0$, the average of total resource consumption tends to infinity:

$$W(0) \rightarrow \infty.$$

This shows the importance of considering a truncated policy as (6).

Comparison to an approximation: It is possible to obtain an approximation for the average amount of resource consumption, denoted by W^{app} . Given that all BSs remain active during network transmissions, the average resource consumption is obtained by considering a typical Voronoi cell \mathcal{V}_0 . As such, we need to compute the average of needed resources in the cell \mathcal{V}_0 . One conventional way is thus to compute the average bandwidth consumption for a single UE, and then multiply that with the average number of UEs located at \mathcal{V}_0 . According to (9), and for path-loss exponent $e = 4$, the average resource consumption for a typical UE located at origin ($\mathbf{x}_0 = \mathbf{0}$) is

$$\bar{w}_0 = \int_0^{w_{\text{th}}} w \frac{d}{dw} \mathbf{F}_{w_0}(w) dw \mathbf{F}_{w_0}(w_{\text{th}}),$$

where

$$\begin{aligned}
\mathbf{F}_{w_0}(w) &= 1 - \mathbb{P} \{ |h_0^0|^2 \|\mathbf{r}_0\|^{-4} \leq I_0 \eta(w) \} \\
&\stackrel{(a)}{=} \mathbb{E}_{I_0, r_0} \{ \exp(-\eta(w) I_0 \|\mathbf{r}_0\|^4) \} \\
&= \mathbb{E}_{\Phi_b, \{h_j^0\}_j, r_0} \left\{ \prod_{j \in \Phi_b \setminus \{0\}} \exp(-\eta(w) |h_j^0|^2 r_j^{-4} r_0^4) \right\} \\
&\stackrel{(b)}{=} \mathbb{E}_{\Phi_b, r_0} \left\{ \prod_{j \in \Phi_b \setminus \{0\}} (1 + \eta(w) r_j^{-4} r_0^4)^{-1} \right\} \\
&\stackrel{(c)}{=} \mathbb{E}_{r_0} \left\{ \exp \left(2\pi \lambda_b \int_{r_0}^\infty ((1 + \eta(w) r^{-4} r_0^4)^{-1} - 1) r dr \right) \right\} \\
&= \mathbb{E}_{r_0} \left\{ \exp \left(-\pi \lambda_b r_0^2 \sqrt{\eta(w)} \tan^{-1}(\sqrt{\eta(w)}) \right) r dr \right\} \\
&\stackrel{(e)}{=} \frac{1}{1 + \sqrt{\eta(w)} \tan^{-1}(\sqrt{\eta(w)})},
\end{aligned}$$

with $I_0 = \sum_{j \in \Phi_b \setminus \{0\}} |h_j^0|^2 \|\mathbf{r}_j\|^{-4}$ being the interference power experienced by UE 0. Moreover, for (a) and (b), we used $|h_0^0|^2 \sim \exp(1)$ and $|h_j^0|^2 \sim \exp(1)$, and we set $r_0 = \|\mathbf{r}_0\|$ and $r_j = \|\mathbf{r}_j\|$, for (c), we leveraged Campbell's Theorem [21], for (d), we exploited the PDF of r_0 : $f(r_0) = 2\pi \lambda_b r_0 \exp(-\pi \lambda_b r_0^2)$.

On the other hand, based on (4), the average number of UEs in the cell \mathcal{V}_0 is $\bar{n}_u = \frac{\lambda_u}{\lambda_b}$. Therefore, we can get:

$$\begin{aligned}
W^{\text{app}}(\gamma) &= \bar{n}_u \bar{w}_0 \\
&= \frac{\lambda_u}{\lambda_b} \int_0^{w_{\text{th}}} w \frac{d}{dw} \left(\frac{1}{1 + \sqrt{\eta(w)} \tan^{-1}(\sqrt{\eta(w)})} \right) dw \\
&\quad \times \frac{1}{1 + \sqrt{\gamma} \tan^{-1}(\sqrt{\gamma})},
\end{aligned} \tag{14}$$

Therefore, equation (14) presents an approximation of exact value of network-wide average resource consumption (8). **Remark:** While equations (8) and (14) demonstrate resource consumption proportionate to λ_u/λ_b , the dependency on γ differs between them.

Figures 1 and 2 compare the approximation W^{app} (14) and the exact value W (8) of network-wide resource consumption as a function of SINR service threshold γ for $R \in \{1, 10, 100\}$ Kbps and $\lambda_u/\lambda_b = 10$. This result highlights the difference between W^{app} and W , particularly for high and low values of γ . However, despite this variance, the approximation remains acceptable for moderate values of γ .

IV. CONCLUSION

In this paper, we developed two identities related to Poisson Point Processes and Poisson-Voronoi tessellation. We then presented some applications of these identities. One application was related to the computation of resource consumption for the conventional transmission scheme in cellular networks. The results showed the versatility of derived identities in analysis

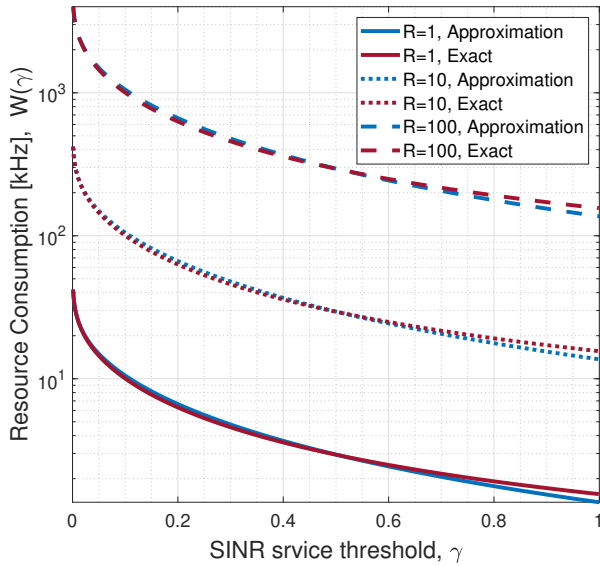


Fig. 1: Comparison between approximation $W^{\text{app}}(\gamma)$ and exact $W(\gamma)$ values as a function of SINR service threshold γ .

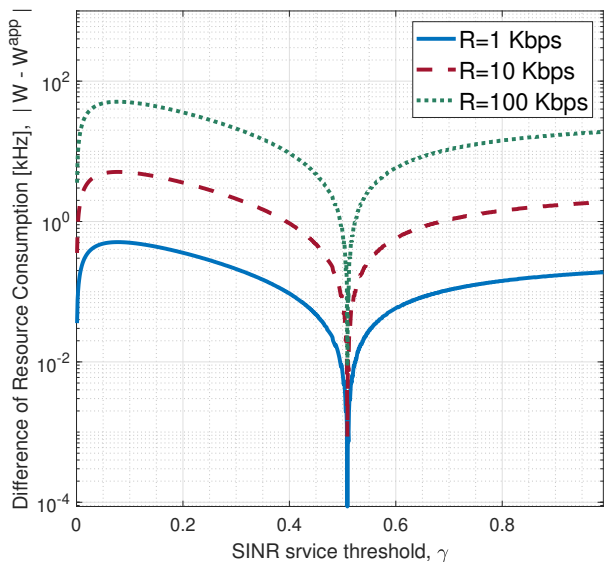


Fig. 2: Difference between approximation $W^{\text{app}}(\gamma)$ and exact $W(\gamma)$ values as a function of SINR service threshold γ .

of cellular networks. Analysis of network performances for beamforming-based transmission schemes is considered as a future work.

REFERENCES

- [1] J. G. Andrews, F. Baccelli, and R. K. Ganti, "A tractable approach to coverage and rate in cellular networks," *IEEE Transactions on Communications*, vol. 59, no. 11, pp. 3122–3134, 2011.
- [2] F. Baccelli and B. Blaszczyszyn, "Stochastic geometry and wireless networks, volume I: Theory," *Found. Trends Netw.*, vol. 3, no. 3-4, pp. 249–449, 2009.
- [3] —, "Stochastic geometry and wireless networks, volume II: Applications," *Found. Trends Netw.*, vol. 3, no. 3-4, pp. 249–449, 2009.
- [4] H. S. Dhillon, R. K. Ganti, F. Baccelli, and J. G. Andrews, "Modeling and analysis of K-tier downlink heterogeneous cellular networks," *IEEE*

- Journal on Selected Areas in Communications*, vol. 30, no. 3, pp. 550–560, 2012.
- [5] M. Haenggi and R. Ganti, "Interference in large wireless networks," *Found. Trends Netw.*, vol. 3, pp. 127–248, 01 2009.
- [6] H.-S. Jo, Y. J. Sang, P. Xia, and J. G. Andrews, "Heterogeneous cellular networks with flexible cell association: A comprehensive downlink SINR analysis," *IEEE Transactions on Wireless Communications*, vol. 11, no. 10, pp. 3484–3495, 2012.
- [7] J. G. Andrews, A. K. Gupta, and H. S. Dhillon, "A primer on cellular network analysis using stochastic geometry," preprint ArXiv 1604.03183, Apr. 2016.
- [8] M. Amidzadeh, H. Al-Tous, O. Tirkkonen, and G. Caire, "Cellular network caching based on multipoint multicast transmissions," in *IEEE Global Communications Conference (GLOBECOM)*, Dec. 2020, pp. 1–6.
- [9] —, "Orthogonal multipoint multicast caching in OFDM cellular networks with ICI and IBI," in *Proc. IEEE Annu. Int. Symp. Pers. Indoor, Mobile Radio Commun.*, 2021, pp. 394–399.
- [10] M. Amidzadeh, H. Al-Tous, G. Caire, and O. Tirkkonen, "Caching in cellular networks based on multipoint multicast transmissions," *IEEE Trans. Wireless Commun.*, pp. 1–19, 2022.
- [11] M. Amidzadeh, H. Al-Tous, O. Tirkkonen, and G. Caire, "Cellular traffic offloading with optimized compound single-point unicast and cache-based multipoint multicast," in *IEEE Wireless Communications and Networking Conference (WCNC)*, 2022, pp. 2268–2273.
- [12] N. Lee, D. Morales-Jimenez, A. Lozano, and R. W. Heath, "Spectral efficiency of dynamic coordinated beamforming: A stochastic geometry approach," *IEEE Transactions on Wireless Communications*, vol. 14, no. 1, pp. 230–241, 2015.
- [13] J. Wu, B. Chen, C. Yang, and Q. Li, "Caching and bandwidth allocation policy optimization in heterogeneous networks," in *IEEE International Symposium on Personal, Indoor and Mobile Radio Communications PIMRC*, Oct. 2017, pp. 1–6.
- [14] C. Ye, Y. Cui, Y. Yang, and R. Wang, "Optimal caching designs for perfect, imperfect, and unknown file popularity distributions in large-scale multi-tier wireless networks," *IEEE Transactions on Communications*, vol. 67, no. 9, pp. 6612–6625, 2019.
- [15] X. Xu and M. Tao, "Analysis and optimization of probabilistic caching in multi-antenna small-cell networks," in *IEEE Global Communications Conference (GLOBECOM)*, 2017, pp. 1–6.
- [16] M. Choi, A. F. Molisch, D.-J. Han, D. Kim, J. Kim, and J. Moon, "Probabilistic caching and dynamic delivery policies for categorized contents and consecutive user demands," *IEEE Transactions on Wireless Communications*, vol. 20, no. 4, pp. 2685–2699, 2021.
- [17] B. Serbetci and J. Gosling, "On optimal geographical caching in heterogeneous cellular networks," in *IEEE Wireless Communications and Networking Conference (WCNC)*, March. 2017, pp. 1–6.
- [18] E. Pineda, V. Garrido, and D. Crespo, "Domain-size distribution in a poisson-voronoi nucleation and growth transformation," *Phys. Rev. E*, vol. 75, p. 040107, Apr 2007.
- [19] D. Cao, S. Zhou, and Z. Niu, "Optimal base station density for energy-efficient heterogeneous cellular networks," in *IEEE International Conference on Communications (ICC)*, 2012, pp. 4379–4383.
- [20] F. Baccelli and B. Blaszczyszyn, "Stochastic geometry and wireless networks, volume 1: Theory," *Found. Trends Netw.*, vol. 3, no. 3-4, pp. 249–449, 2009.
- [21] J. Kingman, *Poisson Processes*. Oxford, England: Oxford University Press, 1993.
- [22] J. Wen, K. Huang, S. Yang, and V. O. K. Li, "Cache-enabled heterogeneous cellular networks: Optimal tier-level content placement," *IEEE Transactions on Wireless Communications*, vol. 16, no. 9, pp. 5939–5952, 2017.
- [23] K. Li, C. Yang, Z. Chen, and M. Tao, "Optimization and analysis of probabilistic caching in N-tier heterogeneous networks," *IEEE Transactions on Wireless Communications*, vol. 17, no. 2, pp. 1283–1297, 2018.
- [24] J. Wu, C. Yang, and B. Chen, "Proactive caching and bandwidth allocation in heterogeneous networks by learning from historical numbers of requests," *IEEE Transactions on Communications*, vol. 68, no. 7, pp. 4394–4410, 2020.
- [25] F. Rusek, D. Persson, B. K. Lau, E. G. Larsson, T. L. Marzetta, O. Edfors, and F. Tufvesson, "Scaling up MIMO—opportunities and challenges with very large arrays," *IEEE Signal Process. Mag.*, vol. 30, no. 1, pp. 40–60, 2013.

- [26] J. Laiho, A. Wacker, and T. Novosad, *Radio Network Planning and Optimisation for UMTS*. John Wiley & Sons, 2006.
- [27] L. Garcia, K. Pedersen, and P. Mogensen, "Autonomous component carrier selection: Interference management in local area environments for LTE-advanced," *IEEE Commun. Mag.*, vol. 47, no. 9, pp. 110–116, 2009.
- [28] A. Goldsmith, *Wireless Communications*. Cambridge, UK: Cambridge University Press, 2005.
- [29] S. N. Chiu, D. Stoyan, W. S. Kendall, and J. Mecke, *Stochastic Geometry and Its Applications*, 3rd ed. John Wiley & Sons, 2013.

APPENDIX

A. Proof of Lemma 1

Let N denote the number of points of Φ_1 , which follows a Poisson distribution. Suppose that the points are placed in the region A as a subspace of Cartesian space. Note that for a homogeneous PPP, the points are independently and uniformly distributed within A [29]. We then have:

$$\begin{aligned} \mathbb{E}\left\{\prod_{k \in \Phi} P(\mathbf{x}_k) \sum_{k \in \Phi} S(\mathbf{x}_k)\right\} &= \mathbb{E}_N\left\{\mathbb{E}\left\{\sum_{k=1}^N S(\mathbf{x}_k) P(\mathbf{x}_k) \prod_{i \neq k} P(\mathbf{x}_i) \middle| N\right\}\right\} \\ &\stackrel{(a)}{=} \mathbb{E}_N\left\{\sum_{n=1}^N \iint_A \frac{S(\mathbf{s})P(\mathbf{s})}{|A|} d\mathbf{s} \left(\iint_A \frac{P(\mathbf{s})}{|A|} d\mathbf{s}\right)^{N-1}\right\} \\ &= \iint_A \frac{S(\mathbf{s})P(\mathbf{s})}{|A|} d\mathbf{s} \mathbb{E}_N\left\{N \left(\iint_A \frac{P(\mathbf{s})}{|A|} d\mathbf{s}\right)^{N-1}\right\} \\ &\stackrel{(b)}{=} \iint_A \frac{S(\mathbf{s})P(\mathbf{s})}{|A|} d\mathbf{s} \lambda_1 |A| \exp(-\lambda_1 |A|) \exp\left(\lambda_1 |A| \iint_A \frac{P(\mathbf{s})}{|A|} d\mathbf{s}\right) \end{aligned}$$

where $|A|$ is the area of A , for (a) we consider that points are independently and uniformly distributed over A , and for (b) we use $N \sim \text{Pois}(\lambda_1 |A|)$. By rearranging the last equation and letting $A = \mathbb{R}^2$, the statement follows.

B. Proof of Lemma 2

The first statement 1 follows based on the geometrical definition of the Voronoi tessellation of Φ_2 and definition of $M_0(\cdot)$. For the second statement 2, we consider the given $\mathbf{x} \in \mathbb{R}^2$. Then, we exclude from the Euclidean space the area where $\mathbf{x} \notin M_0(\mathbf{r})$. The resulting area will be equal to a circle centered at \mathbf{x} with radius $\|\mathbf{x}\|$, which is the definition of $B_c(\mathbf{r}; \mathbf{x}, \|\mathbf{x}\|)$. See Figure 3 for an illustration.

C. Proof of Remark 1

$$\begin{aligned} \mathbb{E}\left\{\sum_{k \in \mathcal{V}_0} P(\mathbf{x}_k)\right\} &= \mathbb{E}\left\{\sum_{k \in \Phi_1} P(\mathbf{x}_k) \mathbb{1}(\mathbf{x}_k \in \mathcal{V}_0)\right\} \\ &= \mathbb{E}_{\Phi_1, \Phi_2}\left\{\sum_{k \in \Phi_1} \prod_{j \in \Phi_2 \setminus \{0\}} P(\mathbf{x}_k) \mathbb{1}(\mathbf{x}_k \in M_0(\mathbf{r}_j))\right\} \\ &= \mathbb{E}\left\{\sum_{k \in \Phi_1} P(\mathbf{x}_k) \exp\left(\lambda_2 \iint (\mathbb{1}(\mathbf{x}_k \in M_0(\mathbf{r})) - 1) d\mathbf{r}\right)\right\} \\ &= \mathbb{E}\left\{\sum_{k \in \Phi_1} P(\mathbf{x}_k) \exp\left(\lambda_2 \iint_{B_c(\mathbf{r}, \mathbf{x}_k, \|\mathbf{x}_k\|)} 1 d\mathbf{r} - \lambda_2 \iint_{\mathbb{R}^2} 1 d\mathbf{r}\right)\right\} \\ &= \mathbb{E}\left\{\sum_{k \in \Phi_1} P(\mathbf{x}_k) \exp\left(-\pi \lambda_2 \|\mathbf{x}_k\|^2\right)\right\} \\ &= \lambda_1 \iint P(\mathbf{x}) \exp\left(-\pi \lambda_2 \|\mathbf{x}\|^2\right) d\mathbf{x}, \end{aligned}$$

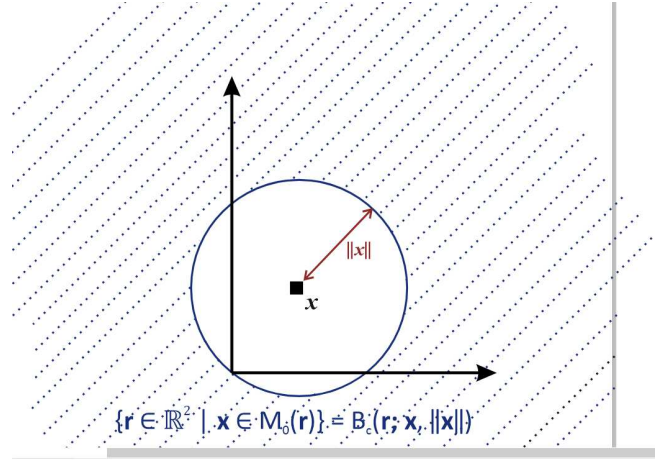


Fig. 3: Illustration of $B_c(\mathbf{r}; \mathbf{x}, \|\mathbf{x}\|)$.

where obtained based on the Campbell theorem, and considering that the distribution of reduced-palm process (when dealing with $\Phi_2 \setminus \{0\}$) is equal to the distribution of original process. In a similar way, it can be shown that:

$$\mathbb{E}\left\{\prod_{k \in \mathcal{V}_0} P(\mathbf{x}_k)\right\} = \exp\left(\lambda_1 \iint_{\mathbb{R}^2} (P(\mathbf{x}) \exp(-\pi \lambda_2 \|\mathbf{x}\|^2) - 1) d\mathbf{x}\right).$$